Radiocarbon in the Eastern Tropical Pacific: Implications for Changes in Equatorial Undercurrent Velocity and Decadal Variability

Lauren B. Kuntz* and Daniel P Schrag[1]

[1]Department of Earth and Planetary Sciences, Harvard University, Cambridge, MA 02138

*Correspondence to: lkuntz2013@gmail.com

Key Points

- **A model of equatorial transport and mixing simulates radiocarbon variability, as observed in coral records**
- **Changes in the velocity of the equatorial undercurrent are a dominant mechanism of radiocarbon variability on decadal timescales**

Abstract

A coral record of radiocarbon variability in seawater from the Galapagos shows a step change in radiocarbon values across the 1976 climate shift, associated with a similar rise in sea surface temperature during the season of maximum upwelling. We present a simple model of water transport and mixing in the equatorial Pacific that is used to simulate radiocarbon variability to compare with the coral data. The results indicate that the velocity of the Equatorial Undercurrent (EUC) is the dominant mechanism responsible for the pattern of variability observed in the coral record, suggesting that decadal variability in the EUC may be an important component of decadal variability in Pacific and global temperature.

Plain Language Summary

The aboveground testing of nuclear weapons during the 1950s created a sudden increase of radiocarbon in the atmosphere. The penetration of this signal into the ocean provided researchers with a novel dataset offering insights into circulation patterns. Here, we focus on understanding variability in the radiocarbon signal from coral records along the equatorial Pacific. We find that variations in equatorial circulations may be important to explaining both the radiocarbon signal as well as decadal variability in Pacific and global temperature.

1 Introduction

On interannual and decadal timescales, variability in the equatorial Pacific is strongly associated with global temperature changes (e.g. *Mantua et al*, 1997; *Zhang et al*, 1997; *Cayan et al*, 2001; *Patt and Gwata*, 2002; *Kosaka and Xie*, 2013; *Deutsch et al,* 2014). In particular, a warming of sea-surface temperatures (SSTs) in the equatorial Pacific in 1976, termed the 1976 Pacific climate shift, has been linked to major atmosphere and oceanic changes sustained for decades (e.g. *Graham,* 1994; *Trenberth and Hoar*, 1996; *Rajagopalan et al*, 1997; *Deser et al*, 2004). A number of ideas have been proposed to explain this shift, ranging from anomalously warm subsurface waters from the North Pacific (*Gu and Philander*, 1997), to anomalous water flux transport (*Kleeman et al*, 1999), and changes in the relative contribution of northern and southern hemisphere waters (*Guilderson and Schrag*, 1998; *Rodgers et al,* 1999). Identifying the mechanism behind the 1976 shift remains an important approach to exploring how the Earth system responds to rising greenhouse gas concentrations (*Broecker*, 2017).

Synchronized with the 1976 shift in SSTs**,** Guilderson and Schrag (1998) noted an abrupt increase in radiocarbon (^{14}C) content of the surface waters in the equatorial Pacific, particularly during the season of strongest upwelling (Fig. 1). They speculated that the shift was caused by a decrease in contribution of radiocarbon-depleted deeper waters to the upwelling region, or a change in the structure of the ventilated thermocline. In this study, we explore the origin of the 1976 shift in radiocarbon using a simple box model of the equatorial Pacific. Using winds and velocities in the equatorial undercurrent (EUC) to drive upwelling and shear-induced mixing respectively, we explore the impact each has on the climatology and variability of the radiocarbon signal. We find that changes in

EUC velocity dominate the radiocarbon signal and discuss the implications for other climate shifts observed in the equatorial Pacific.

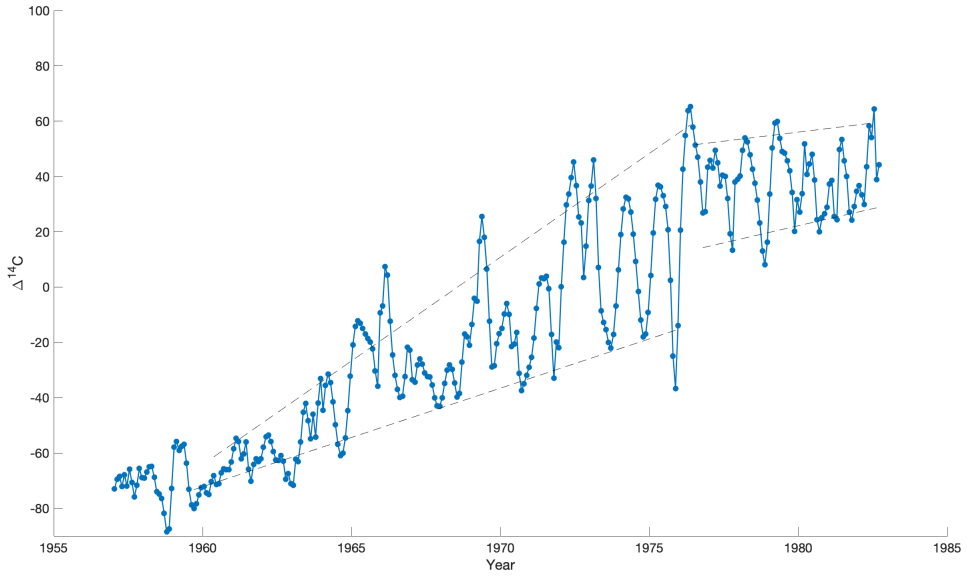

Figure 1. Galapagos coral $\Delta^{14}C$ record (Fig. 1 from *Guilderson and Schrag*, 1998). Linear trend lines of upwelling and non-upwelling season extremes pre and post 1976 are shown (dashed lines).

2 Materials and Methods

Our model of the eastern equatorial Pacific consists of two and a half layers of unit width and length: a surface layer, thermocline layer, and deep ocean layer of infinite depth. The model calculates the concentration of dissolved inorganic carbon (DIC) and radiocarbon in the surface and thermocline layers for monthly time steps over the length of the Galapagos record.

The concentrations of DIC and radiocarbon (C_{surf}) in the surface ocean evolve as

$$C_{surf}(t) = \left\{ \frac{v_{Ekman} + w_{mix}}{H_{surf}} C_t(t-1) + \frac{1 - v_{Ekman} - w_{mix}}{H_{surf}} C_{surf}(t-1) + \frac{F_{invasion}(t) - F_{outgas}(t) - F_{bio}}{H_{surf}} \right\} dt$$

The first term on the right hand side reflects the upwelling of thermocline waters (with concentration C_t) due to both Ekman pumping (v_{Ekman}) and shear induced mixing (w_{mix}). The second term is the export of surface waters due to meridional Ekman divergence (v_{Ekman}) and downward shear induced mixing (w_{mix}). Additional fluxes from air-sea gas exchange ($F_{invasion}$ and F_{outgas}) as well as biological consumption (F_{bio}) are also included. We calculate the concentration by normalizing the fluxes by the depth of the surface layer (H_{surf}). Because the zonal gradient in carbon and radiocarbon is minimal in the eastern equatorial Pacific, the zonal advection of surface water is assumed to have negligible

impact. It is possible that during very strong El Niño events, some water from the Western Pacific moves eastward into the upwelling region, but this is an unusual occurrence. As the focus of this paper is on the overall pattern of radiocarbon variability and especially the minimum values, this assumption is not important to our result.

In the thermocline, the concentrations of carbon and radiocarbon (C_t) are calculated as

$$C_t(t) = \left\{ \frac{H_t - w_{mix} - w_{deep} - v_{Ekman}}{H_t} C_{EUC}(t-1) + \frac{w_{mix}}{H_t} C_{surf}(t-1) + \frac{w_{deep}}{H_t} C_{deep} \right\} dt$$

The first term reflects the replenishment of thermocline waters with waters from the EUC, accounting for losses due Ekman pumping, and mixing with the surface and waters at depth (w_{deep}). The second and last terms account for the mixing of surface waters downward and deep waters upward respectively. We calculate the concentration by normalizing the fluxes by the depth of the thermocline layer (H_t).

The net flux from air-sea gas exchange depends on the partial pressure of CO_2 in the ocean and atmosphere (pCO_2)

$$F_{invasion}(t) - F_{outgas}(t) = kK_o \left(pCO_2^{ATM} - pCO_2^{surf} \right)$$

K_o is the solubility of CO_2, calculated at each time step following the empirical relationship from Weiss (1974). We calculate the gas transfer velocity, k, using Wanninkhof's (1992) parameterization

$$k = 0.31u^2 \left(\frac{660}{Sc} \right)^2$$

where u is the 10m wind speed, taken as the average over the eastern equatorial Pacific from the ECMWF twentieth century reanalysis (ERA-20C) (*Poli et al*, 2016), and *Sc* is the Schmidt number (*Wang et al,* 2006). The details of the air-sea gas exchange parameterization are not important to the overall result. We assume salinity to be constant at 34.78 per mil, and use temperatures in the Nino 3 region from the Global Ocean Surface Temperature Atlas (GOSTA) dataset (*Bottomley et al*, 1990).

We use measurements from Mauna Loa to prescribe the partial pressure of CO_2 in the atmosphere at each time step (*Keeling et al*, 2001). These data being in 1958, so we assume the first year of the simulation (1957) has a partial pressure equal to the average of the 1958 measurements. Because the air-sea gas exchange is a small carbon flux for the eastern Pacific compared to the other fluxes, the errors this causes should be minor. At each time step, we prescribe the partial pressure of radiocarbon in the atmosphere along the equator as the average of radiocarbon in the Northern Hemisphere (Vermunt, Austria) (*Levin et* al, 1994) and Southern Hemisphere (Wellington, New Zealand) (*Manning and Melhuish*, 1994). We ignore any fractionation that could occur in the air-sea gas exchange.

We use zonal wind stress from ERA-20C to calculate Ekman pumping, which drives both divergence and upwelling.

129 $$v_{Ekman} = \frac{1}{\rho f}\frac{\partial \tau^x}{\partial y}$$

130 We combined divergence from the northern and southern hemispheres, using the
131 difference in wind stress along the equator (-5 to 5N, 180 to 240E) and in the subtropics
132 (25 to 35N/S, 180 to 240E) to calculate the meridional gradient in wind stress.
133
134 The Richardson number, which is a measure of mixing, is proportional to the square of
135 vertical shear. We parameterize mixing with both the surface and deep water through this
136 relationship, using the EUC velocity at 220E (where the current is strongest) and
137 assuming the vertical extent of the current is symmetric and does not change.
138 $$w_{mix} = w_{deep} \propto v_{EUC}^2$$
139 Because there are no direct measurements of the EUC velocity in situ over this period, we
140 explore 3 different prescriptions: an empirical relationship with Nino3.4 region
141 temperatures derived from a linear fit of CESM (Community Earth System Model from
142 NCAR) model simulations, output from the Simple Ocean Data Assimilation reanalysis
143 (SODA) (*Carton and Giese*, 2008), and output from the Ocean Reanalysis System
144 (ORAS) (*Mogensen et al*, 2012; *Balmaseda et al*, 2013). For each EUC prescription, we
145 calculate a constant of proportionality between the undercurrent and mixing by fitting the
146 model to replicate the magnitude and seasonal variability of carbon and radiocarbon
147 under pre-bomb, climatological conditions.
148
149 The radiocarbon in the EUC changes over time due to the delayed bomb signal. Surface
150 waters in the northern and southern subtropics subduct and propagate through the
151 ventilated thermocline before feeding into the EUC (e.g. *Luyten et al*, 1983; *Tsuchiya et*
152 *al*, 1989; *Rodgers et al*, 2003; *Kuntz and Schrag*, 2018). To reflect this transport, which
153 both delays and smooths the bomb radiocarbon signal due to advection timescales along-
154 isopycnal mixing respectively, we prescribe the EUC radiocarbon content to be a lagged,
155 weighted average from northern and southern signals.
156 $$^{14}C_{EUC}(t) = 0.2\,^{14}\overline{C}_{NP}(t - 2\text{years}) + 0.8\,^{14}\overline{C}_{SP}(t - 2\text{years})$$
157 where the over bar reflects a 12 year average, and the weights come from the dominance
158 of southern hemisphere waters in the EUC (*Kuntz and Schrag*, 2018). The values of
159 radiocarbon in each hemisphere come from coral records from Rarotonga (21S, 159W)
160 (*Guilderson et al*, 2000) and the French Frigate (24N, 166W) (*Druffel*, 1987), assuming a
161 DIC concentration of 2.0 mol/kg.
162
163 We parameterize a number of model values. In the deep ocean, we set the DIC to 2.2
164 mol/kg (*Chai et al*, 2002) with a $\Delta^{14}C$ of -95‰ to reflect pre-bomb levels (*Broecker et al*,
165 1985). The DIC of the EUC is held constant at 2.05 mol/kg and biological uptake in the
166 surface is fixed to be 8×10^{-4} mol C/m^3/day (*Chai et al*, 2002). We set the depth of the
167 surface and thermocline boxes to 25 m. None of these choices significantly affect the
168 results presented here. Detailed sensitivity analyses for variations in surface layer
169 thickness, DIC content (both in the EUC and in deeper water), pre-bomb radiocarbon,
170 and biological productivity are shown in the Supplement, but none of these have a
171 significant influence on the results presented below.
172

We initialized the model with a DIC in the surface of 2.0 mol/kg, and radiocarbon equivalent to the start of the Galapagos record.

3 Results

The model simulation for surface DIC and $\Delta^{14}C$ pre-bomb, climatological conditions shows regular fluctuations with seasonal variations in DIC from 1.98 to 2.01 mmol and $\Delta^{14}C$ from -80‰ to a maximum just over -78‰ (see Supplement), consistent with minimal variation of pre-bomb $\Delta^{14}C$ from Galapagos Corals (Guilderson and Schrag, 1998). Figure 2 shows the model simulation with the delayed signal of bomb radiocarbon and using Nino3.4 temperatures to parameterize the EUC velocity. Constant wind stress and constant EUC velocities recreate the initial increase and post 1976 plateau of radiocarbon but fail to capture the seasonal and interannual variability (Fig. 2A). Adding the climatological winds and EUC velocities creates a seasonal cycle, but the amplitude is diminished compared to observations (Fig. 2B). Including the time evolving wind stress has minimal impact on the model simulation of radiocarbon (Fig. 2C). Only when a time evolving undercurrent is included does the simulation display variability similar to observations (Fig. 2D). In this case, the linear trend in radiocarbon pre-1976 is greater in the non-upwelling than upwelling season, but both trends decrease post-1976. There is also a distinct jump in the upwelling season $\Delta^{14}C$ values, analogous to the observations.

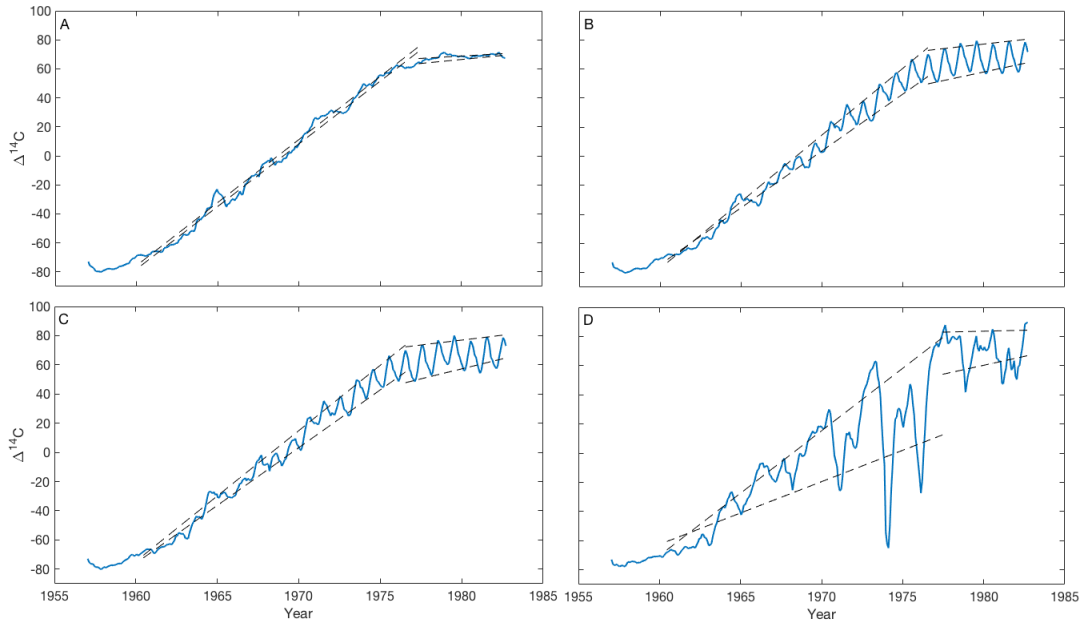

Figure 2. Model simulation of Galapagoes radiocarbon with the delayed signal of bomb radiocarbon in the EUC and using Nino3.4 temperatures to parameterize the EUC velocities. Four simulations are shown: constant wind stress and EUC velocities (A), climatological wind stress and EUC velocities (B), time-evolving wind stress and climatological EUC velocities (C), and time-evolving wind stress and EUC velocities (D). As in Guilderson and Schrag (1998) linear trend lines of upwelling and non-upwelling season extremes pre and post 1976 are shown (dashed lines).

Different prescriptions for EUC velocity yield very different radiocarbon results (Fig. 3). Model calculations taking EUC velocities from each of the reanalysis ocean models (SODA and ORAS) fail to reproduce the jump in minimum value of $\Delta^{14}C$ observed in the data. Only the Nino3.4 empirical relationship fit for EUC velocity reproduces the step change in minimum radiocarbon values in 1976.

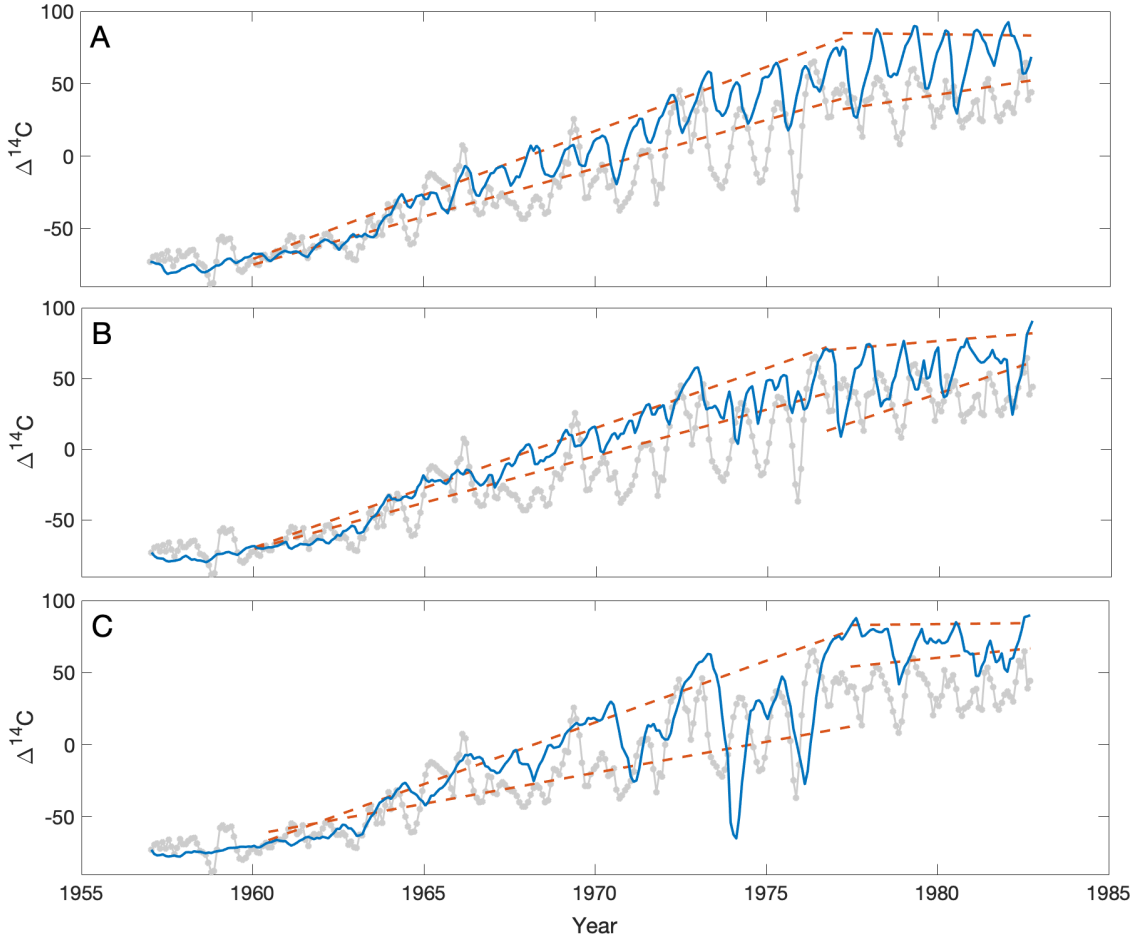

Figure 3. Galapagos radiocarbon from model simulations with EUC velocities from the SODA reanalysis (A), the ORAS reanalysis (B), and the Nino3.4 empirical relationship (C). As in Guilderson and Schrag (1998) linear trend lines of upwelling and non-upwelling season extremes pre and post 1976 are shown (dashed, red lines). Observations are shown in gray.

4 Discussion

Our simple model for radiocarbon in the eastern equatorial Pacific can be used to diagnose the importance of different physical mechanisms to the signal observed in the coral record from the Galapagos. The magnitude of the pre-bomb radiocarbon seasonal cycle agrees with the variability seen in the first two years of the Galapagos record, although the absolute values are slightly more depleted. The simulations during the bomb era show the importance of the EUC velocity to reproducing the jump in miminum $\Delta^{14}C$ values seen in the Galapagos coral. The variability in seasonal maximum and minimums stems from changes in EUC strength and shear induced mixing (Fig. 2).

Changes in wind stress do not appear to be a primary control on the radiocarbon signal, as climatological winds and observed winds show similar results (Figs. 2B and 2C). Only the calculation with EUC velocities tied to Niño3.4 temperature (Fig. 2D) is able to reproduce the shift in minimum $\Delta^{14}C$ seen across the 1976 transition, although the amplitude of the seasonal and interannual variability in the model is greater than what is seen in the coral record. Prior to 1976, a faster EUC induced greater mixing with deeper, radiocarbon-depleted water along the EUC pathway, resulting in lower seasonal minima. After 1976, a reduction in average EUC velocity led to less mixing and lower dilution of the bomb signal, leading to a jump in the seasonal minima in $\Delta^{14}C$. Such a shift in EUC velocity is also consistent with the jump in SST minima in the Nino3 region post-1976 (*Guilderson and Schrag*, 1998), although the sensitivity to EUC velocity is greater for radiocarbon because of the large contrast in vertical distribution of radiocarbon.

An interesting feature of this analysis is that neither of the two reanalysis products shows EUC variability compatible with the radiocarbon record. Only the Niño3.4 empirical parameterization of EUC velocities reproduces the 1976 shift. The empirical relationship between Niño3.4 temperature and EUC velocity comes from a linear correlation of monthly EUC velocity in the CESM model (r=-0.67; see Supplement), and may capture decadal variability better than the reanalysis products.

Our simple model indicates that the critical features of the Galapagos radiocarbon record are driven primarily by EUC velocity, in particular that the shift in 1976 represents a reduction in the EUC strength. Around the turn of the 21st century, the eastern equatorial Pacific temperatures experienced a shift in the opposite direction, reversing the 1976 shift (e.g. *Ding et al*, 2013; *Trenberth et al*, 2014). If our analysis of the radiocarbon record is correct, this implies an acceleration of the EUC around 2000. Observations confirm this, revealing an acceleration of the EUC around the transition of the eastern equatorial Pacific to a cold phase (*Amaya et al*, 2015; *Coats and Karnauskas, 2018*). We see this even more clearly in an analysis of the TAO array data from 220°E (ref) that show a significant jump in average EUC velocity around the time of the transition to more stable global temperatures (Figure 4). Combined with the radiocarbon evidence from the 1976 shift, these data emphasize the importance of understanding controls on EUC velocity to explaining and predicting decadal changes in tropical Pacific and global temperature.

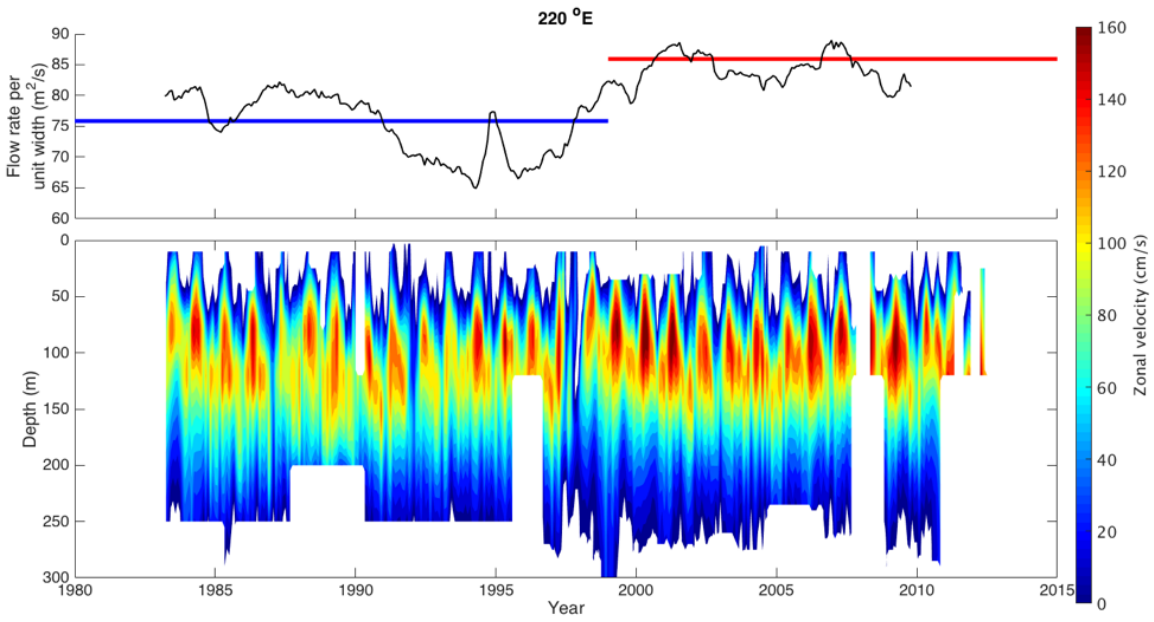

Figure 4 Zonal velocity along the equator from the TAO buoy at 140°W, using both acoustic Doppler current profilers and current meter data (TAO Project Office, 2000). To focus on the EUC, only positive (eastward) zonal velocities are shown in the contour plot. An increase in current strength is evident post 1999. The line plot highlights this change, showing average flow rate per unit width above 80 cm/s before and after 1999, as well as the 5-year running mean (black). The record from the 110°W buoy shows a similar signal, but the records from the other TAO buoys are not complete enough to perform this analysis.

5 Conclusions

A simple model for radiocarbon in the eastern equatorial Pacific shows that the velocity of the Equatorial Undercurrent (EUC) is the dominant mechanism behind the evolution of radiocarbon in the sea surface, as recorded by a Galapagos coral. Using an empirical estimate for EUC variability based on eastern equatorial Pacific sea surface temperatures, the model successfully recreates the jump in radiocarbon during the maximum upwelling season across the 1976 climate shift. After 1976, the average velocity of the EUC is reduced, leading to higher radiocarbon values and less cold water in the eastern equatorial Pacific. A similar shift but in the opposite direction around 1999 to 2001 is observed through direct measurements of EUC velocity from a TAO mooring, suggesting that such decadal variability in EUC velocity may be an important mechanism for modulating Pacific and global temperature.

Acknowledgments, Samples, and Data

This material is based upon work supported by a National Science Foundation Graduate Research Fellowship (Grant Number DGE1144152) to LBK and a Star Family Challenge Grant to DPS. Data from the Tropical Atmosphere Ocean Project can from the TAO Project Office of NOAA/PMEL. Data are available in the in-text data citation references: Galapagoes coral record: *Guilderson and Schrag* (1998); French Frigate coral record: *Druffel* (1987), Rarotonga coral record: *Guilderson et al* (2000), atmospheric radiocarbon

at Vermunt, Austria: *Levin et al* (1994), atmospheric radiocarbon at Wellington, New Zealand: *Manning and Melhuish* (1994), atmospheric CO_2: *Keeling et al* (2001), ocean temperature: *Bottomley et al* (1991), atmospheric wind stress from reanalysis: *Poli et al* (2016), equatorial velocities from ocean reanalysis: *Carton and Giese* (2008), *Mogensen et al* (2012) and *Balmaseda et al* (2013). Code used for the model and data analysis is available at doi: 10.5281/zenodo.4302802

References

Amaya, D. J, Xie, S.-P., Miller, A. J., & McPhaden, M. J. (2015), Seasonality of tropical Pacific decadal trends associated with the 21st century global warming hiatus. *Journal of Geophysical Research: Oceans*, 120, 6782-6798. doi:10.1002/2015JC01906

Balmaseda, M. A., Trenberth, K. E., & Källén, E. (2013). Distinctive climate signals in reanalysis of global ocean heat content. *Geophysical Research Letters,* 40, 1-6. doi.org:10.1002/grl.50382

Bottomley M., C. K. Folland, J. Hsiung, R. E. Newell, & Parker, D. E. (1990), Global ocean surface temperature atlas "GOSTA". Meteorological Office, Bracknell, UK and the Department of Earth, Atmospheric and Planetary Sciences, Massachusetts Institute of Technology, Cambridge, MA, USA. 20 pp and 313 plates.

Broecker, W. S., Peng, T.-H., Ostlund, G., and Stuiver, M. (1985), The distribution of bomb radiocarbon in the ocean. *Journal of Geophysical Research*, 90, 6953-6970. doi:10.1029/JC090iC04p06953

Broecker, W. (2017), When climate change predictions are right for the wrong reasons. *Climatic Change*, 142**,** 1–6 doi:10.1007/s10584-017-1927-y

Carton, J.A. & Giese, B.S. (2008), A Reanalysis of Ocean Climate Using Simple Ocean Data Assimilation (SODA). *Monthly Weather Review*, 136, 2999-3017. doi:10.1175/2007MWR1978.1

Cayan, D.R., Kammerdiener, S., Dettinger, M.D , Caprio, J.M. & Peterson, D.H. (2001), Changes in the onset of spring in the western United States. *Bulletin of the American Meteorological Society*, 82(3), 399-415. doi.org:10.1175/1520-0477(2001)082<0399:CITOOS>2.3.CO;2

Coats, S., & Karnauskas, K. B. (2018), A role for the equatorial undercurrent in the ocean dynamical thermostat. *Journal of Climate,* 31, 6245-6261. https://doi.org/10.1175/JCLI-D-17-0513.1

Chai, F., Dungdale, R.C., Peng, T.-H., Wilkerson, F. P., & Barber, R. T. (2002), One-dimensional ecosystem model of the equatorial Pacific upwelling system. Part I: Model development and silicon and nitrogen cycle. *Deep Sea Research Part II: Topical Studies in Oceanography*, 49, 2713-2745. doi:10.1016/S0967-0645(02)00055-3.

Deser, C., Phillips, A.S., & Hurrell, J.W. (2004), Pacific interdecadal climate variability: Linkages between the tropics and the North Pacific during boreal winter since 1900. *Journal of Climate*, 17, 3109–3124, doi:10.1175/1520-0442(2004)017<3109:PICVLB>2.0.CO;2

Deutsch, C., Berelson, W., Thunell, R., Weber, T., Tems, C., McManus, J., Crusius, Ito, T., Baumgartner, T., Ferreira, V., Mey, J., & van Geen, A. (2014). Centennial

changes in North Pacific anoxia linked to tropical trade winds. *Science,* 345(6197), 665-668. doi:10.1126/science.1252332

Ding, H., Greatbatch, R.J., Latif, M., Park. W., & Gerdes, R. (2013). Hindcast of the 1976/77 and 1998/99 climate shifts in the Pacific. *Journal of Climate*, 26, 7650-7661. doi:10.1175/JCLI-D-12-00626.1

Druffel, E.R.M. (1987), Bomb radiocarbon in the Pacific: Annual and seasonal timescale variations. *Journal of Marine Research*, 45(3), 667-698. doi:10.1357/002224087788326876

Graham, N. E. (1994), Decadal-scale climate variability in the tropical and North Pacific during the 1970s and 1980s: observations and model results, *Climate Dynamics*, 10, 135–162, doi:10.1007/BF00210626

Gu, D., & Philander, S. G. H. (1997). Interdecadal climate fluctuations that depend on exchanges between the tropics and extratropics. *Science,* 275, 805-807. https://doi.org/ 10.1126/science.275.5301.805.

Guilderson, T. P., & Schrag, D. P. (1998). Abrupt shift in subsurface temperatures in the tropical Pacific associated with changes in El Nino. *Science,* 281, 240-243. https://doi.org/10.1126/science.281.5374.240.

Guilderson, T., Schrag, D., Goddard, E., Kashgarian, M., Wellington, G., & Linsley, B. (2000). Southwest Subtropical Pacific Surface Water Radiocarbon in a High-Resolution Coral Record. *Radiocarbon*, 42(2), 249-256. doi:10.1017/S0033822200059051

Keeling, C. D. , Piper, S. C., Bacastow, R. B., Wahlen, M., Whorf, T. P., Heimann, M. & Meijer, H. A. (2001). Exchanges of atmospheric CO2 and 13CO2 with the terrestrial biosphere and oceans from 1978 to 2000. I. Global aspects, *SIO Reference Series*, No. 01-06, Scripps Institution of Oceanography, San Diego, 88 pages, 2001. http://escholarship.org/uc/item/09v319r9

Kleeman, R., McCreary, J. P., & Klinger, B. A. (1999). A mechanism for generation ENSO decadal variability. *Geophysical Research Letters,* 26, 1743-1746. doi:0.1029/1999GL900352.

Kosaka, Y., & Xie, S. P. (2013). Recent global-warming hiatus tied to equatorial Pacific surface cooling. *Nature,* 501, 403-407. doi:10.1038/nature12534.

Kuntz, L. B., & Schrag, D. P. (2018). Hemispheric asymmetry in the ventilated thermocline of the tropical pacific. *Journal of Climate*, 31, 1281-1288. doi:10.1175/JCLI-D-17-0686.1

Levin, I., Kromer, B., Schoch-Fischer, H., Bruns, M., Münnich, M., Berdau, D., Vogel, J.C., & Münnich, K.O. (1994), δ14CO2 record from Vermunt. *In Trends: A Compendium of Data on Global Change*. Carbon Dioxide Information Analysis Center, Oak Ridge National Laboratory, U.S. Department of Energy, Oak Ridge, Tenn., U.S.A.

Luyten, J.R., Pedlosky, J. & Stommel, H. (1983) The Ventilated Thermocline. *Journal of Physical Oceanography*, 13, 292–309, doi:10.1175/1520-0485(1983)013<0292:TVT>2.0.CO;2

Manning, M.R., & Melhuish, W.H. (1994), Atmospheric δ14C record from Wellington. *In Trends: A Compendium of Data on Global Change.* Carbon Dioxide Information Analysis Center, Oak Ridge National Laboratory, U.S. Department of Energy, Oak Ridge, Tenn., U.S.A.

Mantua, N.J., Hare, S.R., Zhang, Y., Wallace, J.M. & Francis, R.C. (1997), A Pacific interdecadal climate oscillation with impacts on salmon production. *Bulletin of the American Meteorological Society*, 78, 1069–1080, doi:10.1175/1520-0477(1997)078<1069:APICOW>2.0.CO;2

Mogensen, K., Balmaseda, M.A., & Weaver, A.T. (2012), The NEMOVAR ocean data assimilation system as implemented in the ECMWF ocean analysis for System 4. *Technical Memorandum*. 668. ECMWF: Reading, UK.

Patt, A. and Gwata, C. (2002) Effective Seasonal Climate Forecast Applications: Examining Constraints for Subsistence Farmers in Zimbabwe. *Global Environmental Change*, 12, 185-195. doi:10.1016/S0959-3780(02)00013-4

Poli, P., Hersbach, H. , Dee, D.P., Berrisford, P., Simmons, A.J., Vitart, F., Laloyaux, P., Tan, D.G., Peubey, C., Thépaut, J., Trémolet, Y., Hólm, E.V., Bonavita, M., Isaksen, L., and Fisher, M., (2016) ERA-20C: An Atmospheric Reanalysis of the Twentieth Century. *Journal of Climate*, 29, 4083–4097, doi:10.1175/JCLI-D-15-0556.1

Rajagopalan, B., Lall, U., & Cane, M.A. (1997) Anomalous ENSO occurences: An alternative view. *Journal of Climate*, 10, 2351-2357. doi:10.1175/1520-0442(1997)010<2351:AEOAAV>2.0.CO;2

Rodgers, K. B., Cane, M. A., Naik, N. H., & Schrag, D. P. (1999). The role of the Indonesian throughflow in equatorial Pacific thermocline ventilation. *Journal of Geophysical Research: Oceans*. 104, 20551-20570, doi:10.1029/1998JC900094.

Rodgers, K. B., Blanke, B., Madec, G., Aumont, O., Ciais, P., & Dutay, J.-C. (2003). Extratropical sources of equatorial Pacific upwelling in an OGCM. *Geophysical Research Letters,* 30, 1084. doi:10.1029/2002GL016003.

Trenberth, K. E., & Hoar, T. J. (1996), The 1990-1995 El Nino-Southern Oscillation event: Longest on record. *Geophysical Research Letters*, 23(1), 57-60. doi:10.1029/95GL03602

Trenberth, K.E., Fasullo, J.T., Branstator, G., & Phillips, A.S. (2014) Seasonal aspects of the recent pause in surface warming. *Nature Climate Change*, 4, 911-916. doi:10.1038/NCLIMATE2341

Tsuchiya, M., Lukas, R., Fine, R. A., Firing, E., & Lindstrom, E. (1989). Source waters of the Pacific Equatorial Undercurrent. *Progress in Oceanography*, 23(2), 101-147. doi:10.1016/0079-6611(89)90012-8

Wanninkhof, R. (1992), Relationship between gas exchange and wind speed over the ocean, *Journal of Geophysical Research*, 97(C5), 7373–7381, doi:10.1029/92JC00188.

Wang, X., Christian, J. R., Murtugudde, R., & Busalacchi, A.J. (2006). Spatial and temporial variability of the surface water pCO2 and air-sea CO2 flux in the equatorial Pacific during 1980-2003: A basin-scale carbon cycle model. *Journal of Geophysical Research*, 111, C07S04, doi: 10.1029/2005JC002972

Weiss, R.F. (1974) Carbon dioxide in water and seawater: the solubility of a non-ideal gas. *Marine Chemistry*, 2(3), 203-215. doi:10.1016/0304-4203(74)90015-2.

Zhang, Y., Wallace, J.M., & Battisti, D.S. (1997). ENSO-like interdecadal variability: 1900-93. *Journal of Climate*, 10, 1004-1020, doi:10.1175/1520-0442(1997)010<1004:ELIV>2.0CO;2